Science in China Series D: Earth Sciences

Wave energy input into the Ekman layer

WU KeJian†, YANG ZhongLiang, LIU Bin & GUAN ChangLong

Physical Oceanography Laboratory, Ocean University of China, Qingdao 266100, China

This paper is concerned with the wave energy input into the Ekman layer, based on 3 observational facts that surface waves could significantly affect the profile of the Ekman layer. Under the assumption of constant vertical diffusivity, the analytical form of wave energy input into the Ekman layer is derived. Analysis of the energy balance shows that the energy input to the Ekman layer through the wind stress and the interaction of the Stokes-drift with planetary vorticity can be divided into two kinds. One is the wind energy input, and the other is the wave energy input which is dependent on wind speed, wave characteristics and the wind direction relative to the wave direction. Estimates of wave energy input show that wave energy input can be up to 10% in high-latitude and high-wind speed areas and higher than 20% in the Antarctic Circumpolar Current, compared with the wind energy input into the classical Ekman layer. Results of this paper are of significance to the study of wave-induced large scale effects.

Ekman layer, wind energy input, wave energy input

Since the surface mixed layer plays an important role in the coupling between the atmosphere and ocean, energetics of ocean circulation associated with wind energy flux to the surface mixed layer have taken on community interests in the past. Faller[1] first discussed the energetics of ocean circulation from wind stress, tidal dissipation and other sources. The global wind energy flux to inertial motions was estimated at 0.47—0.7 TW by Watanabe and Hibiya[2] and Alford[3]. Wunsch[4] and Huang et al.[5] made an estimate of the wind energy to geostrophic current at 1 TW. Wang and Huang[6] employed the classical Ekman model to estimate global wind energy input to the subinertial motions as 2.3—2.4 TW. Attempt to estimate the wind energy flux to surface waves has also been made recently by Wang and Huang[7] (60 TW). However, in the above-mentioned studies, energy inputs to currents and surface waves were discussed independently. Whether or not the surface waves could have influences on wind energy input to the currents remains unclear.

The classical Ekman theory, assuming a balance between Coriolis force and the divergence of momentum transfer by turbulence stress, predicted a perfect current profile of Ekman spiral. However, observational evidence did not directly support the classical Ekman model. There are three features that cannot be predicted by the Ekman model. Firstly, the surface current lies at an angle between 10° and 45° to the surface wind stress[8].Cushman-Roisin[9] documented a smaller angle ranging from 5° to 10°. Secondly, at a depth between 5 and 20 m the current is deflected by approximately 75° from the wind stress[10]. Thirdly, the current is rapidly attenuated below the surface[10].

Advances have been made recently in tackling the above-mentioned discrepancies between theory and observations. Recent studies show that the key to understanding the observed Ekman current profiles is the influence of surface wave motion via the Stokes-drift[11,12]. The interaction between the Coriolis force and the Stokes drift associated with ocean surface waves leads to a vertical transport, which can be expressed as a force on

Received April 9, 2007; accepted July 27, 2007
doi: 10.1007/s11430-007-0147-0

†Corresponding author (email: kejianwu@ouc.edu.cn)

Supported by the National Basic Research Program of China (973 program) (Grant Nos. 2005CB422302 and 2007CB411806) and the Major Project of the National Natural Science Foundation of China (Grant No. 40490263)

the mean momentum equation in the direction along wave crests[13−15]. By incorporating this wave-induced Coriolis-Stokes forcing into the momentum balance of the Ekman layer, the analytical solution is shown to agree reasonably well with current profiles from observations and certainly agrees much better than the classical Ekman model[11,12]. The wind work on the Ekman layer comes directly from the wind stress acting on the sea surface. This energy input depends not only on the wind stress vector but also on the current profiles. The importance of surface waves in determining the current profiles leads to an intuitive idea that surface waves would also affect the wind energy input to the Ekman layer.

The aim of this paper is to investigate influences of surface waves on the wind energy input to the so-called Ekman-Stokes layer.

1 Energetics of the Ekman-Stokes Layer

1.1 Energy balance

To investigate the wave effects on wind energy input to the Ekman layer, it is important to include the effect of surface waves in the momentum equation. By using scales analysis, Webber and Melson[16] derived the wave-filtered momentum equation that waves affect the mean motions primarily through the wave-induced Coriolis-Stokes forcing. McWilliams et al.[17] also obtained the same results. The Coriolis-Stokes forcing can be written as $-\hat{z}f\times U_{\mathrm{s}}$, where $\hat{z}$ is the unit vector directed upward, f is the Coriolis parameter, and U_s is the Stokes-drift produced by surface waves. For a monochromatic deep water wave with wave amplitude a, wavenumber k and frequency σ, the Stokes-drift profile associated with such a wave is[18]

$$U_{\mathrm{s}}=U_{\mathrm{s,\,s}}\mathrm{e}^{2kz}\hat{k}\,,\quad U_{\mathrm{s,\,s}}=a^2\sigma k, \tag{1}$$

where $\hat{k}$ is the unit wavenumber vector, and $U_{s,s}$ is the velocity of Stokes-drift at sea surface. Note that the Stokes depth scale is $d_{\mathrm{s}}=1/(2k)$, with a typical value of 5—10 m.

With the wave-induced Coriolis-Stokes forcing included, the momentum equation describing the non-steady-state, ageostrophic current in the surface layer is[11,12,17]

$$\frac{\partial U}{\partial t}+f\,\hat{z}\times\left(U+U_{\mathrm{s}}\right)=\frac{\partial}{\partial z}\left(A_z\frac{\partial U}{\partial z}\right), \tag{2}$$

where the coordinate is set on the mean, zero water level, $U=(u, v)$ is the horizontal current, A_z is the vertical momentum diffusivity, and t is time.

This Ekman layer including Stokes-drift can be called the Ekman-Stokes layer[12]. It satisfies the following boundary conditions:

$$\rho_{\mathrm{w}}A_z\frac{\partial U}{\partial z}=\tau,\ \text{at}\ z=0;\ U\to 0,\ \text{as}\ z\to-\infty, \tag{3}$$

where ρ_{w} is water density and τ is wind stress. Multiplying eq. (2) by $\rho_{\mathrm{w}}U$ and integrating from $z=-\infty$ to z=0 leads to the energy balance

$$\frac{\mathrm{d}E}{\mathrm{d}t}=E_{\mathrm{w}}+E_{\mathrm{s}}-D, \tag{4}$$

where

$$E=\rho_{\mathrm{w}}\int_{-\infty}^{0}\frac{1}{2}|U|^2\,\mathrm{d}z,\quad E_w=\tau\cdot U(0),$$

$$E_{\mathrm{s}}=\rho_{\mathrm{w}}\int_{-\infty}^{0}\left(-f\,\hat{z}\times U_{\mathrm{s}}\right)\cdot U\mathrm{d}z,\quad \text{and}\ D=\rho_{\mathrm{w}}\int_{-\infty}^{0}A_z\left|\frac{\partial U}{\partial z}\right|^2\mathrm{d}z \tag{5}$$

represent the total kinetic energy of the Ekman-Stokes layer, the rate of wind energy input, the rate of energy input caused by the interaction of Stoke-drift with planetary vorticity, and the dissipation rate, respectively. Note that the energy input E_{w} is from the direct action of wind stress. Compared with the energy balance of the classical Ekman model[6], a new term of energy input E_{s}, which can be called the wave-induced energy input, is introduced into the energy balance because of the Coriolis-Stokes forcing. In this paper, we strictly distinguish the energy input, E_{s}, work done directly by the Coriolis-Stokes forcing, from the wind energy input E_{w}. Since the Coriolis-Stokes forcing is originated from the wind-generated waves, the energy input E_{s} can be considered as a part of indirect work done by the wind stress.

For the steady-state Ekman layer, $E_{\mathrm{w}}+E_{\mathrm{s}}=D$, i.e., the energy input is balanced by dissipation. In the pure Ekman layer, the wind energy input sustains the turbulence and mixing in the upper ocean.

1.2 The steady solution

If assuming a constant vertical diffusivity and using the complex notation to re-express the variables $U=(u, v)$, $U_{\mathrm{s}}=(u_{\mathrm{s}}, v_{\mathrm{s}})$ and $\tau=(\tau_x, \tau_y)$ as $U=u+iv$, $U_{\mathrm{s}}=u_{\mathrm{s}}+iv_{\mathrm{s}}$ and $\tau=\tau_x+i\tau_y$, respectively, the steady-state solution to eq. (2) can be easily written as

$$U = W_e + W_{es} + W_s, \quad (6)$$

$$W_e = \frac{\tau}{\rho_w A_z j} e^{jz}, \quad W_{es} = -\frac{2kjU_s(0)}{(2k)^2 - j^2} e^{jz},$$

$$W_s = \frac{j^2 U_s(0)}{(2k)^2 - j^2} e^{2kz}. \quad (7)$$

Here $j=(1+i)/d$, $d = \sqrt{2A_z/f}$. Note that eq. (7) is applicable for both the Northern Hemisphere ($f > 0$) and Southern Hemisphere ($f < 0$). The depth of the Ekman layer, d_e, is defined as

$$d_e = \sqrt{\frac{2A_z}{|f|}}. \quad (8)$$

Note that the first term W_e is the pure Ekman solution when the wave-induced effects were not included. However, the second term W_{es} and third term W_s are the two new terms introduced by the Coriolis-Stokes forcing. Arising as a particular solution to the Coriolis-Stokes forcing, W_s decays over the Stokes depth scale d_s. Importantly, there is an Ekman-Stokes component of the current W_{es}. This term decays over the Ekman depth scale, d_e, and so changes the current profile through the whole depth of the Ekman layer.

Since both of the two new terms of the solution were introduced by inclusion of the Coriolis-Stokes forcing in eq. (2), we have enough reasons to anticipate that they would have important influences on energy inputs to the Ekman-Stokes layer.

1.3 The wind energy input E_w

From the steady solution of the Ekman-Stokes layer, the wind energy input to the mixed layer can be derived. To clearly investigate the wave-induced effects, we split the wind energy input into three terms

$$E_w = E_{w,1} + E_{w,2} + E_{w,3}, \quad (9)$$

where

$$E_{w,1} = \frac{|\tau|^2}{\rho_w d_e |f|}, \quad E_{w,2} = -\tau \cdot U_s(0) f_1(c),$$
$$E_{w,3} = \pm \hat{z} \cdot (\tau \times U_s(0)) f_2(c) \begin{pmatrix} +: f > 0 \\ -: f < 0 \end{pmatrix}, \quad (10)$$

and the two functions $f_1(c)$ and $f_2(c)$ are expressed as

$$f_1(c) = \frac{c+2}{(c+1)^2 + 1}, \quad f_2(c) = \frac{c}{(c+1)^2 + 1}. \quad (11)$$

The non-dimensional parameter c is defined as the ratio of the depth of the Ekman layer to that of the Stokes-drift,

$$c = \frac{d_e}{d_s}. \quad (12)$$

In the present paper, we name the parameter c the Ekman-Stokes depth number in order to distinguish it from the Ekman-Stokes number[19].

Apparently, the wind energy input to the Ekman-Stokes layer consists of three terms. The first term, $E_{w,1}$, is exactly the wind energy input to the pure Ekman layer. Details of this energy input associated with its estimate for the world ocean have been discussed recently by Wang and Huang[6]. The second and third parts, however, are two new terms that were introduced into the wind energy input because of inclusion of the Coriolis-Stokes forcing. Both of them are functionally dependent not only on the Ekman-Stokes depth number, but also on the angle between the Stokes-drift and wind stress. The smaller the angle, the smaller the contribution paid by the third term ($E_{w,3}$) to the wind-induced energy input. Notice that, if the wind stress is oriented perpendicular to right (left) of the direction of the Stokes-drift, the second term ($E_{w,2}$) will vanish and the third term ($E_{w,3}$) will be at its greatest (smallest). Such a case would only occur when a swell propagates over an area where a storm has ever occurred. For simplicity, we make an assumption in this study that the direction of wind stress is exactly the same as that of the Stokes-drift. Although this assumption usually breaks down in the real world ocean, field measurements and numerical ocean wave modeling suggest that the averaged wave direction, hence the Stokes-drift direction, usually lie at a smaller angle to the wind stress.

After making such an assumption, we can see that the third term of wind energy input vanishes, and the second term reduces to

$$E_{w,2} = -|\tau||U_s(0)| f_1(c). \quad (13)$$

There are two limiting cases. Firstly, consider the case when $c \to \infty$, that is, the depth of Ekman layer is much greater than that of the Stokes-drift layer. In this case, the wave-induced term of wind energy input $E_{w,2}$ tends to zero. This corresponds to a case that influences of Coriolis-Stokes forcing on the Ekman layer vanish, and the wind energy input E_w reduces to wind energy input to the pure Ekman layer, $E_{w,1}$.

Secondly, consider the case when c tends to zero; that is, the Ekman layer depth is much smaller than the Stokes-drift depth. As pointed out by Polton et al.[12], in the ocean this regime might represent swell propagation over a shallow wind-driven layer. In this case, the term $E_{2,2}$ reduces to $-|\tau||U_s(0)|$.

1.4 The wave-induced energy input E_s

The wave-induced energy input is also split into three terms:

$$E_s = E_{s,1} + E_{s,2} + E_{s,3}, \quad (14)$$

where

$$E_{s,1} = \rho_w |f| d_s |U_s(0)|^2 f_3(c),\ E_{s,2} = \tau \cdot U_s(0) f_1(c),$$
$$E_{s,3} = \pm \hat{z} \cdot (\tau \times U_s(0)) f_2(c) \begin{pmatrix} +: f > 0 \\ -: f < 0 \end{pmatrix}, \quad (15)$$

and the function $f_3(c)$ is expressed as

$$f_3(c) = \frac{c^2(c^3 - c^2 + 2)}{(c^4 + 4)[(c+1)^2 + 1]}. \quad (16)$$

Again, if assuming that the direction of the wind stress is the same as that of the Stokes-drift, the third term of wave-induced energy input, $E_{s,3}$, vanishes and the second term, $E_{s,2}$, reduces to

$$E_{s,2} = |\tau||U_s(0)| f_1(c). \quad (17)$$

Clearly, for both cases of $c \to \infty$ and $c \to 0$, $E_{s,2}$ tends to zero. If the wind stress lies at an angle to the Stokes-drift, the third term, $E_{s,3}$, will also tend to zero for both cases mentioned above.

The second term of the wave-induced energy input has an opposite magnitude compared with the second term of the wind energy input. It vanishes when $c \to \infty$ and reduces to $E_{s,2} = \tau \cdot U_s(0)$ when $c \to 0$. Physically, in the real ocean when a swell propagates over a shallow wind-driven layer, the wave-induced energy input through Coriolis-Stokes forcing will be the work done by the wind stress directly on the Stokes-drift.

1.5 The total amount of energy input E_{tot}

From expressions of wind energy input and wave-induced energy input discussed above, we can easily obtain the total amount of energy input, so that

$$E_{tot} = E_s + E_w = \frac{|\tau|^2}{\rho_w d_e |f|} + \rho_w |f| d_s |U_s(0)|^2 f_3(c). \quad (18)$$

Apparently, the total energy input only includes the first term of wind energy input, $E_{w,1}$, and the first term of wave-induced energy input, $E_{s,1}$. In comparison with the wind energy input to the pure Ekman layer ($E_{w,1}$), the total energy input to the Ekman-Stokes is increased by $E_{s,1}$. The second term of wind energy input is cancelled by the second term of wave-induced energy input in the total energy input, indicating that both of them has no contribution to the total energy input. Physically, the Coriolis-Stokes forcing not only increases energy input to the Ekman layer, but also plays an important role in transferring the energy input within the mixed layer. Compared with the pure Ekman layer, the reduced part of energy input ($E_{w,2}$) was exactly transferred to be as a part in the wave-induced energy input through the Coriolis-Stokes forcing. For both cases of $c \to \infty$ and $c \to 0$, since $f_3(c) \to 0$, the total amount of energy input becomes the wind energy input to the pure Ekman layer. Thus, whenever $d_e >> d_s$ or $d_e << d_s$, the energy input to the Ekman-Stokes layer by the Coriolis-Stokes forcing can be neglected.

2 Estimates of wave-induced energy input

To estimate wave influences on the energy input, two ratios associated with the wave-induced energy input are considered in this study. The first ratio (R_1) considers a measure of the first term of wave-induced energy input ($E_{s,1}$) compared to the wind energy input into the pure Ekman layer ($E_{w,1}$). This ratio gives how much the energy input to the Ekman layer is increased by inclusion of the Coriolis-Stokes forcing. The second ratio (R_2) compares the transferred energy input by wave-induced effect ($E_{s,2}$) with $E_{w,1}$. This ratio presents how much the wind energy input is reduced in comparison with that to the pure Ekman layer, or, how much energy input is transferred by the Coriolis-Stokes forcing within the Ekman-Stokes layer.

2.1 Ratio of $E_{s,1}$ to $E_{w,1}$

The ratio of the first term of wave-induced energy input to the wind energy input into the pure Ekman layer is given by

$$R_1 = \left(\frac{\rho_w d_s |f||U_s(0)|}{|\tau|} \right)^2 c f_3(c). \quad (19)$$

It can be seen that this ratio depends functionally on magnitudes of both the Stokes-drift and wind stress, the depth of the Stokes-drift and that of the Ekman layer.

Firstly, it seems difficult to estimate the depth of the Ekman layer, since there are no observations for the vertical diffusivity A_z. Conventionally, the Ekman layer depth is expressed as an empirical formula: $d_e=\gamma u_{*w}/f$, where u_{*w} is the turbulent friction velocity in water traditionally defined by $u_{*w} = \sqrt{|\tau|/\rho_w}$, and γ is a non-dimensional constant. Whereas a constant of 0.4 is commonly accepted, a somewhat smaller value of between 0.25—0.4 is also recommended under certain oceanic conditions[9,10]. Using six datasets of observations, Wang and Huang[6] recently suggested a constant of 0.5. In this study, we will use the mean value (γ=0.38) of between 0.25—0.5 to estimate the Ekman layer depth, so that,

$$d_e = 0.38 \frac{u_{*a}}{f} \sqrt{\frac{\rho_a}{\rho_w}}, \qquad (20)$$

where ρ_a is the density of air and u_{*a} is the friction velocity in air.

Secondly, the Stokes-drift is determined by the characteristics of surface waves. Komen et al.[20] gave a series of wave growth equations based on a number of datasets of observations. For simplicity, we assume here that the waves are fully developed. Using the following expressions for a and σ,

$$\frac{g^2 a^2}{4u_{*a}^4} = 1.1\times 10^3, \quad \frac{\sigma u_{*a}}{g} = 2\pi \times 5.6 \times 10^{-3}, \qquad (21)$$

we can obtain the estimate of the Stokes-drift depth and, hence, the Coriolis-Stokes depth number, so that,

$$d_s = \frac{g}{2\sigma^2}, \quad c = \frac{0.76\sigma^2 u_{*a}}{gf} \sqrt{\frac{\rho_a}{\rho_w}}. \qquad (22)$$

Finally, the magnitude of wind stress vector can be expressed in terms of the 10 m wind speed U_{10} and the atmospheric drag coefficient C_D as $|\tau| = \rho_a C_D U_{10}^2$. Since C_D is normally expressed as an empirical function of wind speed U_{10} and the friction velocity u_{*a} is related to C_D by $u_{*a} = \sqrt{C_D} U_{10}$, the ratio R_1 can be estimated directly from the wind speed U_{10}.

Figure 1 shows how R_1 increases with wind speed varying from 1 m s^{-1} to 25 m s^{-1} for 4 different latitudes: 15°, 30°, 45°, 60°. It can be seen that, at mid- or high-latitude areas and for a moderate wind speed of 10 m s^{-1}, the increased energy input induced by wave effects can reach as much as 4%—7% of the wind energy input to the pure Ekman layer. For a higher wind speed like 15 m s^{-1}, this percentage can reach as much as 8%—12%, indicating that the wave-induced energy input cannot be neglected in discussions of energetics of the surface mixed layer.

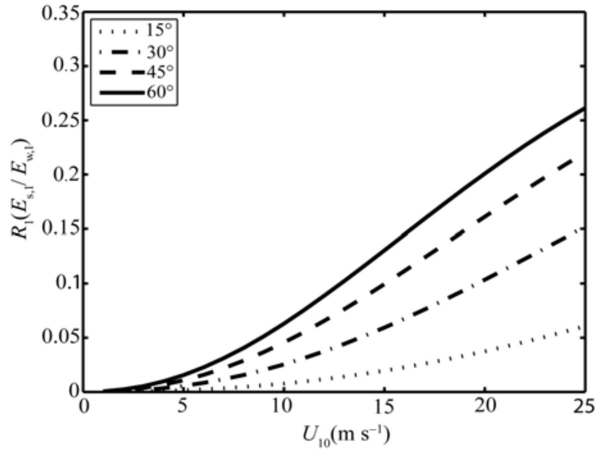

Figure 1 Graph showing how R_1, the ratio of the first term of wave-induced energy input to wind energy input to the pure Ekman layer, varies with wind speed U_{10} for 4 different latitudes: 15°, 30°, 45°, 60°.

2.2 Ratio of $E_{s,2}$ to $E_{w,1}$

The second ratio is given by comparing the second term of wave energy input ($E_{s,2}$) with the wind energy input to the pure Ekman layer ($E_{w,1}$):

$$R_2 = \frac{\rho_w d_e |f||U_s(0)|}{|\tau|} f_1(c). \qquad (23)$$

As discussed above, all quantities of d_e, $|U_s(0)|$, $|\tau|$ and $f_1(c)$ can be inferred from wind speed U_{10}. Thus, the ratio R_2 can also be estimated directly from U_{10} and, hence, we will know the role of the Coriolis-Stokes forcing in transferring the energy input within the Ekman-Stokes layer.

Figure 2 shows how R_2 increases with wind speed for 4 different latitudes: 15°, 30°, 45°, 60°. If taken a latitude of 45° and a wind speed of 10 m s^{-1}, R_2=0.21,

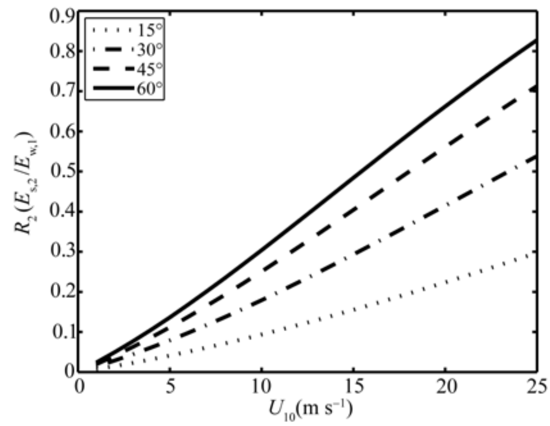

Figure 2 Graph showing how R_2, the ratio of the second term of wave-induced energy input to wind energy input to the pure Ekman layer, varies with wind speed U_{10} for 4 different latitudes: 15°, 30°, 45°, 60°.

indicating that the transferred energy input can be a significant fraction of the wind energy input.

3 Energy input to non-steady Ekman-Stokes layer

3.1 Wind energy input to pure Ekman layer

Using complex variables and the Fourier expansion, $U=u+iv$, $\tau=\tau_x+i\tau_y$, $U=\sum_{-\infty}^{\infty}U_n \mathrm{e}^{i\omega_n t}$, $\tau=\sum_{-\infty}^{\infty}T_n \mathrm{e}^{i\omega_n t}$, $\omega_n=\frac{2\pi}{n}T$, we have the momentum equation for the nth component of current without wave effects included[6],

$$i\left(f+\omega_n\right)U_n=A_z\frac{\mathrm{d}^2U_n}{\mathrm{d}z^2}. \tag{24}$$

The corresponding wind energy input for the nth component is

$$E_{\mathrm{w}}^n=\frac{|T_n|^2}{\rho_{\mathrm{w}}|f+\omega_n|d_{\mathrm{e}}^n}, \tag{25}$$

where $d_{\mathrm{e}}^n=\sqrt{2A_z/|f+\omega_n|}$ is the Ekman layer depth for the nth component. The total amount of wind energy input is

$$E_{\mathrm{w}}=\sum_{n=-\infty}^{\infty}\frac{|T_n|^2}{\rho_{\mathrm{w}}\sqrt{|f(f+\omega_n)|}d_{\mathrm{e}}}. \tag{26}$$

3.2 Energy input to the Ekman-Stokes layer

For calculation of energy input to the Ekman-Stokes layer, we still use the complex variables and the Fourier expansion mentioned above, and represent the Stokes-drift as $U_{\mathrm{s}}=u_{\mathrm{s}}+iv_{\mathrm{s}}=\sum_{-\infty}^{\infty}X_n\mathrm{e}^{i\omega_n t}$. Then, the momentum equation for the nth component of current is

$$i\left(f+\omega_n\right)U_n+ifX_n=A_z\frac{\mathrm{d}^2U_n}{\mathrm{d}z^2}. \tag{27}$$

(i) Wind energy input. The wind energy input for the nth component is

$$E_{\mathrm{w}}^n=\frac{|T_n|^2}{\rho_{\mathrm{w}}d_{\mathrm{e}}^n|f+\omega_n|}-\frac{f}{f+\omega_n}|T_n||X_n(0)|f_1(c_n). \tag{28}$$

(ii) Wave-induced energy input. The wave-induced energy input for the nth component is

$$E_{\mathrm{s}}^n=\rho_{\mathrm{w}}\frac{f^2}{|f+\omega_n|}d_{\mathrm{s}}^n|X_n(0)|^2f_3(c_n)$$

$$+\frac{f}{f+\omega_n}|T_n||X_n(0)|f_1(c_n). \tag{29}$$

(iii) Total energy input. The total energy input for the nth component is

$$E_{\mathrm{tot}}^n=\frac{|T_n|^2}{\rho_{\mathrm{w}}d_{\mathrm{e}}^n|f+\omega_n|}+\rho_{\mathrm{w}}\frac{f^2}{|f+\omega_n|}d_{\mathrm{s}}^n|X_n(0)|^2f_3(c_n). \tag{30}$$

Note that all f in c_n should be replaced by $f+\omega_n$, so that

$$c_n=\frac{d_{\mathrm{e}}^n}{d_{\mathrm{s}}^n}=\frac{d_{\mathrm{e}}}{d_{\mathrm{s}}^n}\sqrt{\frac{|f|}{|f+\omega_n|}}. \tag{31}$$

The amount of total wind and wave-induced energy inputs can be computed by using eqs. (28)—(30).

4 The case of when wind direction does not coincide with wave direction

In the following, we discuss the case of when the wind direction is not the same as that of waves. Based on the above discussions, the wind and waves energy inputs into the Ekman-Stokes layer are, respectively, expressed by

$$E_{\mathrm{w}}=E_{\mathrm{w,1}}+E_{\mathrm{w,2}}+E_{\mathrm{w,3}}, \tag{32}$$

$$E_{\mathrm{w,1}}=\frac{|\tau|^2}{\rho_{\mathrm{w}}d_{\mathrm{e}}|f|},\quad E_{\mathrm{w,2}}=-\tau\cdot U_{\mathrm{s}}(0)f_1(c),$$

$$E_{\mathrm{w,3}}=\pm\hat{z}\cdot\left(\tau\times U_{\mathrm{s}}(0)\right)f_2(c)\begin{pmatrix}+:f>0\\-:f<0\end{pmatrix} \tag{33}$$

$$E_{\mathrm{s}}=E_{\mathrm{s,1}}+E_{\mathrm{s,2}}+E_{\mathrm{s,3}}, \tag{34}$$

$$E_{\mathrm{s,1}}=\rho_{\mathrm{w}}|f|d_{\mathrm{s}}|U_{\mathrm{s}}(0)|^2f_3(c),\ E_{\mathrm{s,2}}=-E_{\mathrm{w,2}},E_{\mathrm{s,3}}=E_{\mathrm{w,3}}. \tag{35}$$

From eqs. (32)—(35), we can obtain the total energy input into the Ekman layer:

$$E_{\mathrm{tot}}=E_{\mathrm{w,1}}+E_{\mathrm{s,1}}+2E_{\mathrm{s,3}}. \tag{36}$$

To consider the waves energy input, we introduce two new ratios R_3 and R_4. R_3 is the ratio of $E_{\mathrm{s,3}}$ to $E_{\mathrm{w,1}}$ and R_4 is the ratio of $E_{\mathrm{s,1}}+2E_{\mathrm{s,3}}$ to $E_{\mathrm{w,1}}$. Ratio R_3 is expressed as

$$R_3=\frac{\rho_{\mathrm{w}}d_{\mathrm{e}}|f||U_{\mathrm{s}}(0)|\sin(\theta)}{|\tau|}F_2(c), \tag{37}$$

and R_4(=R_1+2R_3) can be easily computed from R_1 and R_3, where θ is defined as the angle that the Stokes drift turns to right of the wind stress vector.

Obviously, ratio R_3 gives how much the energy input to the Ekman layer is increased due to the effect of angle

θ. Ratio R_4 gives how much the total energy input is increased for the case when the wind stress is not in the same direction as the Stokes drift, compared with the wind energy input to the pure Ekman layer. It can be seen that these ratios depend functionally on magnitudes of both the Stokes-drift and wind stress, the non- dimensional Ekman-Stokes depth number c and angle θ. To further proceed with the estimates of these ratios, we make a simplifying assumption that the angle θ is limited within –90° and 90°.

Figure 3 (a)—(c) shows, respectively, how R_2, R_3 and R_4 change with wind speeds 1 m s^{-1}—25 m s^{-1} and with θ varying from –90° to 90° (for 45°S latitude). For a fixed wind speed, the transferred energy input between the direct wind energy input and wave-induced one decreases as θ varies from 0° to 90° or to –90°, and reaches its maxima at 0° (Figure 3(a)). There would be no energy transfer when the wind stress is perpendicular to the Stokes drift. For the case of θ=0°, the transferred energy input is much more than the increased energy input due to the wave effects (e.g., for U_{10}=15 m s^{-1}, latitude =45°S, R_1=8%, and R_2=36%). Figure 3(b) shows the effects of θ on the wave-induced energy input. For a fixed wind speed, R_3 decreases as θ varies from –90° to 90°, and it vanishes at θ=0°. Surprisingly, in the Southern Hemisphere, the effects of θ have positive (negative) contributions to the total energy input when the Stokes drift is directed to right (left) of the wind stress vector. In the Northern Hemisphere, the result is opposite to that in the Southern Hemisphere. Figure 3(c) gives the total increased wave-induced energy input compared to the wind energy input to the pure Ekman layer, including the effects of θ. Apparently the total increased energy input can be positive or negative, mostly depending on the relative positions of the Stokes and the wind stress vector. We find that the effects of θ plays a more important role than $E_{w,1}$ does in the total energy input.

5 Concluding remarks

In this paper, the wave-induced Coriolis-Stokes forcing has been introduced into the classical Ekman model to investigate wave-induced influences on wind energy input to the Ekman-Stokes layer. The results show that the wave energy input into the Ekman-Stokes layer can be up to the order of wind energy input into the classical Ekman layer in the high latitudes and high wind speed.

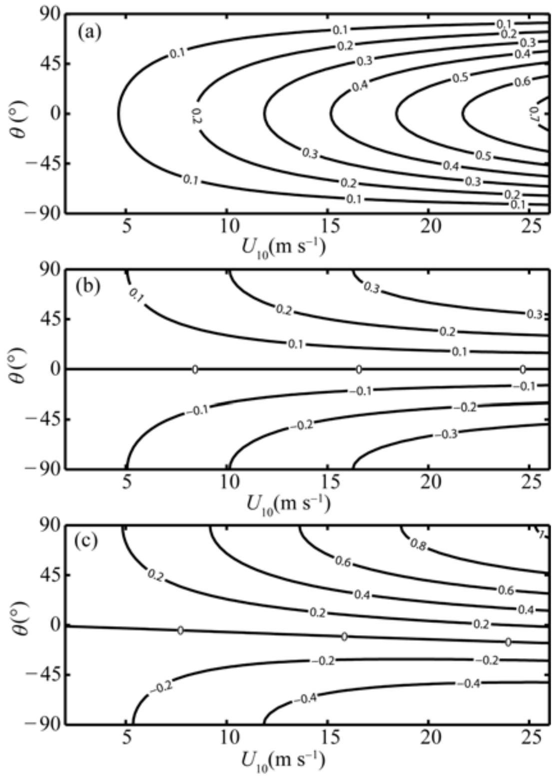

Figure 3 Graph showing how R_2 (a), R_3 (b) and R_4 (c) vary with angle θ and wind speed in the Southern Hemisphere for latitude 45°.

Particularly, in the Antarctic Circumpolar Currents (ACC), the wave energy input can be more than 20% of the wind energy input. Therefore, the surface waves play an important role in discussions of the ocean energy balance in high latitudes.

Incorporation of the Coriolis-Stokes forcing into the momentum balance was found to divide energy input into two kinds. One is the wind energy input (E_w), the other is the wave energy input (E_s) caused by the Coriolis-Stokes forcing, although this energy input is also originated from the wind stress. In the high latitudes and high wind speed areas, the wave energy input to the Ekman layer is significant compared with the wind energy input. McWilliams and Restrepo[19] have studied the wave-driven effects on the ocean circulation from the viewpoint of transport. This paper studied the wave-driven circulation from the viewpoint of energy.

It should be pointed out that only a simple form of constant diffusivity coefficient was considered in this study. For more accurate estimates of the energy inputs to the Ekman-Stokes layer, other forms of diffusivity coefficient varying with water depth should be taken into account. Chen et al.[21] documented a distribution of the so called “swell pools” for the global oceans that there are three swell-dominated zones located in the eastern tropical and subtropical areas of the Pacific, Atlantic and Indian ocean basins. Distribution of the angle between the direction of wave and that of wind stress are shown to be in consistent with distribution of the swell that large angle corresponds to large probability of the swell-dominated. The angle effect is expected to have more influences on the wind-stress energy input in the tropical and subtropical oceans. Therefore, angle effect on the wind-stress energy input should be further examined in specific areas where the swell is dominated.

Another limitation on the application of this study is that the Stokes-drifts were deduced from empirical formulas for fully-developed seas. More accurate calculation of the Stokes-drifts can be predicted from the numerical wave models. This can not only improve accuracy of estimate of the energy inputs, but examine the third term of the wave-induced energy input ($E_{s,3}$) as well.

Discussions with Professor Wei Wang, Physical Oceaography Lab (Ocean University of China), are really appreciated.

1 Faller A J. Sources of energy for the ocean circulation and a theory of the mixed layer. In: Proc Fifth U. S. Congress of Applied Mechanics. Minneapolis, Minnesota, ASME, 1968. 651—762
2 Watanabe M, Hibiya T. Global estimates of the wind-induced energy flux to inertial motions in the surface mixed layer. Geophys Res Lett, 2002, 29: 1239, doi: 10.1029/2001GL014422
3 Alford M H. Improved global maps and 54-year history of wind-work on ocean inertial motions. Geophys Res Lett, 2003, 30: 1424, doi: 10.1029/2002GL016614
4 Wunsch C. The work done by the wind on the oceanic general circulation. J Phys Oceanogr, 1998, 28: 2332—2340[DOI]
5 Huang R X, Wang W, Liu L L. Decadal variability of wind energy to the world ocean. Deep Sea Res II, 2006, 53: 31—41[DOI]
6 Wang W, Huang R X. Wind energy input to the Ekman layer. J Phys Oceanogr, 2004, 34: 1267—1275[DOI]
7 Wang W, Huang R X. Wind energy input to the surface waves. J Phys Oceanogr, 2004, 34: 1276—1280[DOI]
8 Huang N E. On surface drift currents in the ocean. J Fluid Mech, 1979, 91: 191—208[DOI]
9 Cushman-Roisin B. Introduction to Geophysical Fluid Dynamics. New Jersey: Printice-Hall Inc., 1994. 73
10 Price J F, Sundermeyer M A. Stratified Ekman layers. J Geophys Res, 1999, 104: 20467—20494[DOI]
11 Lewis D M, Belcher S E. Time-dependent, coupled, Ekman boundary layer solutions incorporating Stokes drift. Dyn Atmos Oceans, 2004, 37: 313—351[DOI]
12 Polton J A, Lewis D M, Belcher S E. The role of wave-induced Coriolis-Stokes forcing on the wind-driven mixed layer. J Phys Oceanogr, 2005, 35: 444—457
13 Hasselmann K. Wave-driven inertial oscillations. Geophs Fluid Dyn. 1970, 1: 463—502
14 Xu Z G, Bowen A J. Wave- and wind-driven flow in water of finite depth. J Phys Oceanogr, 1994, 24: 1850—1866[DOI]
15 Sun F, Gao S, Wang W, et al. Wave-induced stress and estimation of its driven effect on currents. Sci China Ser D-Earth Sci, 2004, 47: 147—154
16 Webber J K, Melson A. Volme flux induced by wind and waves in a saturated sea. J Geophys Res, 1993, 98: 4739—4745
17 McWilliams J C, Sullivan P P, Moeng C H. Langmuir turbulence in the ocean. J Fluid Mech, 1997, 334: 1—30[DOI]
18 Phillips O M. The Dynamics of the Upper Ocean. Cambridge: Cambridge University Press, 1977. 336
19 McWilliams J C, Restrepo J M. The wave-driven ocean circulation. J Phys Oceanogr, 1999, 29: 2523—2540[DOI]
20 Komen G J, Cavaleri L, Donelan M, et al. Dynamics and Modeling of ocean Waves. Cambridge: Cambridge University Press, 1994. 532
21 Chen G, Chapron B, Ezraty R, et al. A global view of swell and wind sea climate in the ocean by satellite altimeter and scatterometer. J Atmos Oceanic Technol, 2002, 19: 1849—1859[DOI]